JACS
JOURNAL OF THE AMERICAN CHEMICAL SOCIETY
pubs.acs.org/JACS
Communication

Acid-Triggered Side Chain Cleavage Leads to Doped Conjugated Polymers of High Conductivity

Jordan Shanahan, Liang Yan, Yusuf Olanrewaju, Somayeh Kashani, Harald Ade, Franky So, and Wei You*

Cite This: J. Am. Chem. Soc. 2024, 146, 32243−32248
Read Online
ACCESS | Metrics & More | Article Recommendations | Supporting Information

ABSTRACT: Cleavable side chain based conjugated polymers (CSCPs) represent a unique approach to offering solution processability with added benefits via the elimination of insulating side chains. This work highlights an optimally designed polythiophene-carboxylic acid based CSCP, POET-T2-COOH, which achieves a conductivity exceeding 350 S/cm in molecularly doped and side chain cleaved films, 100−100,000 times higher than three other structurally isomeric CSCPs. The high conductivity of POET-T2-COOH is accomplished via a new "cleavage with doping" methodology, synergistically combining a strong acid and a primary dopant. This hybrid method achieves the greatest conductivity in all isomeric CSCPs over conventional doping or cleavage techniques. The doped and side chain cleaved POET-T2-COOH displays a stable conductivity in inert atmospheres and a high work function of 5.3 eV, opening up new applications.

Molecular doping is crucial to increasing charge carrier density (n) and providing tunable conductivity (σ) to conjugated polymers (CPs).[1,2] Although recent works have made breakthroughs in the methodology to dope highly crystalline or polar side chain bearing polymers,[3−9] new strategies to achieve a high yet stable conductivity of doped CPs have stagnated in comparison. Here we utilize cleavable side chain based conjugated polymers (CSCPs) for molecular doping and achieve a 6-order magnitude range in conductivity depending on isomeric structure; further, we discover a new "cleavage with doping" methodology that is superior to other common doping methods. Intuitively, CSCPs are advantageous because they eliminate the insulating side chains in processed CP films. The resulting shorter lamellar spacing can induce less backbone disorder and shorter $\pi-\pi$ stacking, beneficial for higher carrier mobility (μ);[10−12] the concomitant volume reduction also leads to higher n.[13,14] Furthermore, the elimination of soft alkyl chains increases the glass transition of the CP, and remnant carboxylic acids can mitigate destructive oxidation of polymers,[15−19] improving the stability of processed CP film.

We employed the tertiary ester−thiophene motif because it can eliminate side chains and leave behind the carboxylic acid via two different approaches (Scheme S2): (i) direct cleavage between 150 and 220 °C in neat films[16,20] or (ii) acid-induced cleavage at room temperature by soaking films in strong acid (aqueous $pK_a < -10$) solutions,[21] evidenced by Fourier transform infrared (FT-IR) spectroscopy (Figure S9).

Previous works on CPs have shown that additional thiophene units[10,13] and regioregularity[22−24] can maximize the carrier mobility (μ); we thus synthesized four isomeric CSCPs, all containing 50 mol % of tertiary ester−thiophene units and 50 mol % of thiophene units, to explore the relationships between structural design and conductive property (Scheme 1 and Scheme S1). These polymers include regiorandom P3MOCT,[20] regioregular RP-T50,[10] and two new CSCPs named PIET-T2 and POET-T2. The latter two incorporate a twisted inward facing biester thiophene motif (IET) and a planar outward motif (OET), respectively. These orientations (twisted vs planar) have been determined previously in single crystal analysis of similar linear−ester thiophene dimers.[25−27]

We anticipated that the planar OET motif in POET-T2 would minimize the steric hindrance from tertiary carbon in polymer backbones and significantly increase the aggregation behavior; by contrast, the twisted IET motif in PIET-T2 would induce less aggregation. Indeed, POET-T2 is the only polymer that displayed significant temperature-dependent aggregation in its chlorobenzene solution and vibrational peaks in thin film before side chain cleavage (UV/vis spectra, Figures S11 and S13), whereas PIET-T2 shows almost no difference in its absorption profile between solution and thin film.

The difference in positioning of 50 mol % of tertiary ester−thiophene units in these polymers has a strong impact on their energy levels (Figure 1), measured by cyclic voltammetry (CV) (Figure S12). Since all four are structural isomers, the primary influence on the energy levels comes from the planarity of the backbone (i.e., effective conjugation length) and related aggregation behavior. The twisted PIET-T2 possesses the lowest HOMO level at −5.9 eV, and the planar POET-T2 in turn possesses the highest HOMO of −5.5 eV (similar to that of P3HT). The highest HOMO level of POET-

Received: July 19, 2024
Revised: October 13, 2024
Accepted: October 21, 2024
Published: October 28, 2024

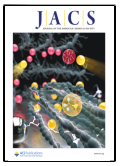

https://doi.org/10.1021/jacs.4c09843
J. Am. Chem. Soc. 2024, 146, 32243−32248

Scheme 1. Isomeric CSCP Structures

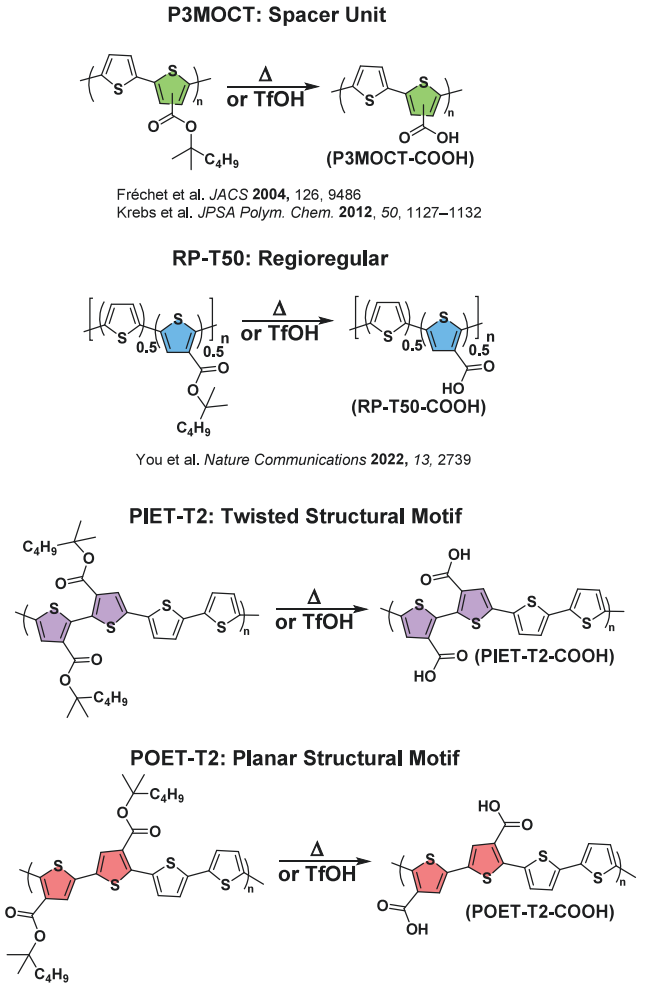

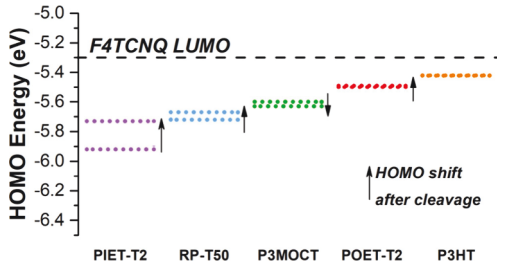

Figure 1. HOMO energy levels for polymers vs the F4TCNQ LUMO energy level (all estimated by CV).

T2 also positions it as the best candidate for efficient doping with F4TCNQ based on energetic alignment, followed by P3MOCT and RP-T50.

While the thermal cleavage of side chains is well documented,[18,28] the acid-triggered cleavage was carried out by dipping the polymer thin film into a moisture exposed triflic acid (TfOH, $pK_a = 0.7$)[29] solution (22.6 mM, 2 μL TfOH in 1 mL acetonitrile) to cleave side chains and form the "CP-COOH" polymer. After acid-triggered cleavage, PIET-T2-COOH shows an increased HOMO level (−5.9 eV → −5.7 eV), likely attributed to a more planar backbone; the other three polymers show very little change in their HOMO levels postcleavage (Figure 1).

We next investigated strategies to combine doping with two different strategies of side chain cleavage. There are two prevailing approaches to incorporate F4TCNQ as the dopant into polymer films: blending dopant into CP solutions then casting film ("blend doping"; 10 wt % of F4TCNQ in here) or dipping films into a solution of dopant ("dip doping"; 3.6 mM of F4TCNQ or 1 mg/mL in acetonitrile). The screened combinations of doping and cleavage methods on the RP-T50 polymer are displayed in Figure 2.

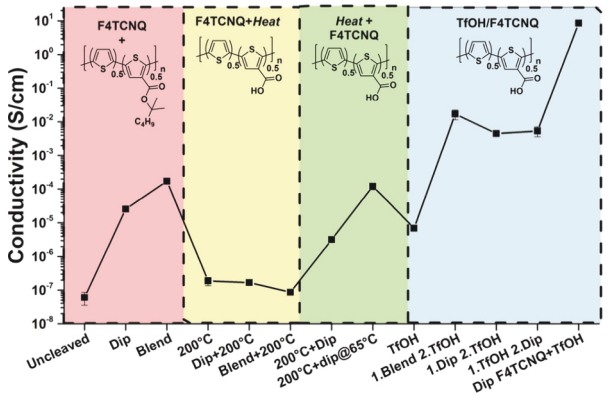

Figure 2. Conductivity vs different cleavage and doping method combinations. All **Dip** conditions indicate dipping in a solution of 3.6 mM F4TCNQ in acetonitrile for 30 min; **200 °C** denotes annealing at 200 °C for 30 min; and **TfOH** indicates dipping in a solution of 22.6 mM TfOH in acetonitrile for 30 min. **1**, **2**, indicate the sequence of methods. **@65 °C** indicates a doping solution at 65 °C for 30 min.

The red shaded region summarizes the key results representative of the F4TCNQ doping of uncleaved RP-T50. The minor doping effect, evidenced by the low σ, is attributed to the low μ of the polymer and low n from poor energy alignment between the polymer and the dopant. Thermolysis at 200 °C (yellow region) results in dedoping of polymer films as F4TCNQ sublimes (Figure S10). Although RP-T50-COOH achieves $10^3\times$ higher μ than the uncleaved RT-T50,[10] subsequent dipping of cleaved films in F4TCNQ results in worse or similar conductivity to the uncleaved polymer, as the dopant is unable to swell into the densified film (green region).

Compared with thermal cleavage, acid-triggered cleavage shows a dramatic difference in conductivity (blue region), depending upon the doping method. First, films subjected to TfOH show acidic protonation-induced doping;[30,31] yet the achieved conductivity is much lower than those of films doped by F4TCNQ first prior to acid-triggered cleavage, which can be ascribed to F4TCNQ's higher electron affinity and faster integer charge transfer mechanism for doping.[32] However, subjecting neat polymer films to a mixed F4TCNQ+TfOH solution caused the conductivity to increase by 10^6 to 8.5 S/cm. We attribute this dramatic increase in part to simultaneous swelling of dopants into polymers during the cleavage process, which can trap dopants after cleaving side chains. By contrast, sequential doping and cleavage would lose dopants by inversed diffusion into the TfOH solution. Interestingly, the UV/vis spectrum of these films (Figure S14c) shows no F4TCNQ radical anion ($F4TCNQ^{\bullet-}$) peaks, which infers an ion exchange of the primary $F4TCNQ^{\bullet-}$ counterion with triflate (TfO^-). This ion exchange was also supported by FT-IR (Figure S23) where the doped films (via mixed F4TCNQ +TfOH) show the absence of F4TCNQ or $F4TCNQ^{\bullet-}$ but

https://doi.org/10.1021/jacs.4c09843
J. Am. Chem. Soc. 2024, 146, 32243−32248

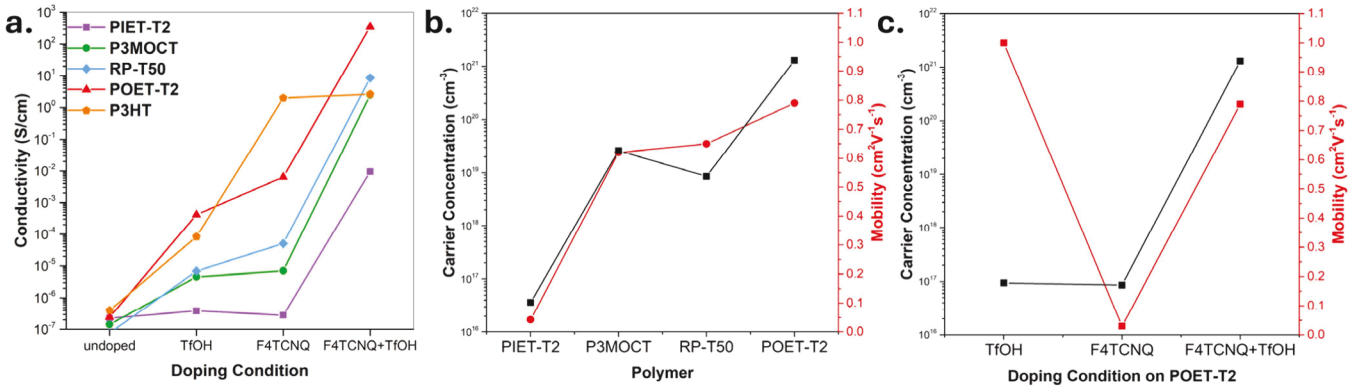

Figure 3. (a) Conductivity of different polymers under different dip doping conditions. (b) Carrier concentration and mobility from the Hall measurement of CSCPs. (c) Carrier concentration and mobility from Hall measurement of POET-T2 vs doping condition.

Table 1. Comparison of Key Parameters of CSCPs with Different Dip Doping Methods

Polymer	TfOH σ^a (S/cm)	F4TCNQ σ^a (S/cm)	F4TCNQ+TfOH σ^a (S/cm)	Hall σ^b (S/cm)	Hall mobility^b ($cm^2\ V^{-1}\ s^{-1}$)	Carrier density^b (cm^{-3})
PIET-T2	$3.81 \times 10^{-7} \pm 7.6 \times 10^{-8}$	$2.81 \times 10^{-7} \pm 5.0 \times 10^{-8}$	$9.54 \times 10^{-3} \pm 1.3 \times 10^{-3}$	2.5×10^{-4}	4.3×10^{-2}	3.6×10^{16}
P3MOCT	$4.52 \times 10^{-6} \pm 6.6 \times 10^{-7}$	$7.06 \times 10^{-6} \pm 1.0 \times 10^{-6}$	2.47 ± 0.40	2.6×10^{0}	6.2×10^{-1}	2.6×10^{19}
RP-T50	$6.92 \times 10^{-6} \pm 6.6 \times 10^{-7}$	$5.00 \times 10^{-5} \pm 4.6 \times 10^{-6}$	8.55 ± 1.56	8.9×10^{-1}	6.5×10^{-1}	8.5×10^{18}
POET-T2	$4.14 \times 10^{-4} \pm 6.4 \times 10^{-5}$	$6.43 \times 10^{-3} \pm 2.4 \times 10^{-4}$	$3.53 \times 10^{2} \pm 2.35 \times 10^{1}$	1.7×10^{2}	7.9×10^{-1}	1.3×10^{21}

[a]Values determined by a two-point probe. [b]Values determined by Hall measurement after the F4TCNQ+TfOH condition. Further discussion of 2-point vs 4-point Hall measurement is in Notes S5 and S6.[35−38]

the presence of TfO^-. This ion exchange process could only occur *after* the doping event (i.e., forming $F4TCNQ^{\bullet-}$) since the NMR results (Figure S22) indicate that neutral F4TCNQ does not react with TfOH. Ion exchange has been demonstrated to effectively increase dopant strength and stability;[5,8,33] additionally, the hydronium adducts formed with F4TCNQ could also account for increased dopant strength.[34]

We next applied the conventional F4TCNQ doping, TfOH cleavage with in situ acid doping ("TfOH" in Figure 3a and Table 1), and the optimized F4TCNQ+TfOH combined condition (which we coin as Acid Cleavage Triggered Via Ion Exchange or ACTVIE) on three other isomeric CSCPs and P3HT. Overall, the same trend prevails for each CP (including P3HT) where F4TCNQ doped films achieve a higher conductivity than the TfOH treated films (Figure 3a). However, no doping of PIET-T2 was observed under either condition since its energetic offset with F4TCNQ is the highest.

ACTVIE doping exhibits an unambiguously large conductivity increase for all CSCPs, with values ranging from 0.0095 S/cm for PIET-T2-COOH to 353 S/cm for POET-T2-COOH. This large range of values reflects the critical importance of optimized polymer structure on achievable conductivity. ACTVIE doped PIET-T2-COOH possesses the lowest μ (almost 10× lower than P3MOCT-COOH) and lowest carrier concentration by the Hall method (Figure 3b and Table 1). Comparison of the regioregular RP-T50-COOH and the regiorandom P3MOCT-COOH reveals a minimal effect of regioregularity on conductivity (σ), where a higher n reflects the higher HOMO level of P3MOCT-COOH and the regioregularity of RP-T50-COOH likely accounts for its higher μ. Furthermore, the ACTVIE doping of P3HT did not result in an increased conductivity over conventional F4TCNQ doping, although it does result in a greater photobleaching of its UV/vis spectra (Figure S14e). This mismatch in bleaching and conductivity could be indicative of destructive side reactions on P3HT,[39] which is not expected for the CSCP-COOHs with oxidation tolerant carboxylates. Additionally, all CSCP-COOHs show incomplete bleaching of their main absorption peak and the rise of a red-shifted polaron/bipolaron band (Figure S14), all *without* $F4TCNQ^{\bullet-}$ absorbance, further supporting the ion exchange and the exclusive high doping efficiency of ACTVIE for CSCPs.

POET-T2 doped through ACTVIE achieves the highest conductivity reported for a polythiophene-carboxylic acid. This is due primarily to the n which exceeds 10^{21} cm^{-3} with an estimated 0.9 carriers on every repeat unit (see Note S4). Further Hall measurements of POET-T2 doped with different methods (Figure 3c and Table S4) show that the ACTVIE condition largely increased the n by over 10^4 higher than TfOH or F4TCNQ doping. Comparing TfOH or F4TCNQ treated films also demonstrates the power of side chain cleavage to increase μ, with TfOH treated films achieving 30× higher μ (1.0 $cm^2\ V^{-1}\ s^{-1}$) than as-cast films doped with F4TCNQ only (0.03 $cm^2\ V^{-1}\ s^{-1}$).

We next employed X-ray photoelectron spectroscopy (XPS) to estimate the doping level, defined as the number of polarons per thiophene ring. Specifically, the ratio of the sulfur in polaron to the sulfur in undoped polymer (Figure S17) can estimate the doping level,[13,40] e.g., 33.6% in the case of ACTVIE doped POET-T2-COOH, much larger than F4TCNQ (11.8%) or TfOH (6.78%). This trend aligns well with the measured conductivity and carrier density. From elemental analysis counts of N 1s to F 1s (Figure S18), we also estimated that the counterion is 90% TfO^- (Note S1). Further, time-of-flight secondary ion mass spectroscopy (ToF-SIMS) measurement (Figure S19) shows that ACTVIE allows dopants to diffuse throughout the entire depth of the polymer thin film.

https://doi.org/10.1021/jacs.4c09843
J. Am. Chem. Soc. 2024, 146, 32243−32248

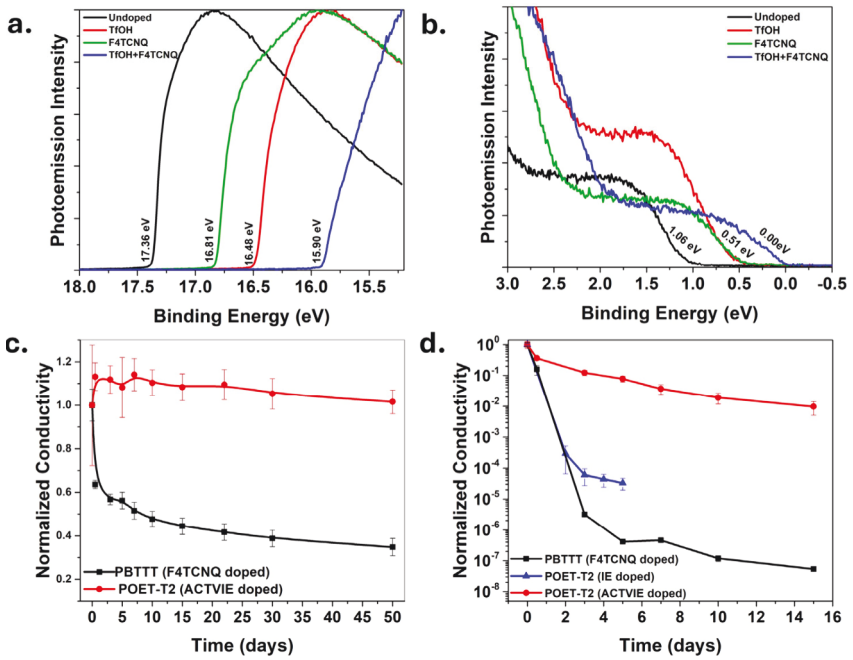

Figure 4. (a) UPS spectra at the Fermi edge and (b) cutoff edge for POET-T2 (or COOH) films after applying different doping methods. Stability measurement for conductivity in an inert glovebox at (c) 25 and (d) 100 °C for ACTVIE doped POET-T2-COOH, F4TCNQ doped PBTTT, and ion exchanged (IE) doped POET-T2 using F4TCNQ and BMP^+TFSI^-.

To highlight the versatility and unique ability of ACTVIE doping of CSCPs, different acid/dopant combinations were tested on POET-T2 (Figures S15 and S16 and Table S5.) Notably, we found that trifluoromethanesulfonimide (pK_a = 0.3 in acetonitrile)[29] could effectively replace TfOH in ACTVIE doping; further, ACTVIE doping achieved higher conductivity than $FeCl_3$ and conventional ion exchange doping.

We also applied ultraviolet photoelectron spectroscopy (UPS) to investigate the change of the Fermi level and work function of doped POET-T2 films. As shown in Figure 4a, 4b, and Table S6, ACTVIE doped POET-T2-COOH exhibits the Fermi level at almost the same energy as its HOMO level, indicative of a metal-like band structure. A work function of 5.32 eV was calculated, noticeably deeper than PEDOT:PSS at 5.0 eV, which could provide a better Ohmic contact in optoelectronics.[41] Unlike conventionally doped alkylated polymers (e.g., PBTTT doped with F4TCNQ), ACTVIE doped POET-T2-COOH possesses excellent solvent resistance (Figure S20) where no decrease in conductivity occurs after soaking films in chloroform, and the stability is much improved with complete retention of conductivity for 50 days in an inert atmosphere (Figure 4c).[42] Additionally, ACTVIE doped POET-T2-COOH showed greater stability than ion exchange doped POET-T2 at 100 °C (Figure 4d), attributed to the cleaved polymer's enhanced thermomechanical properties.[18,43,44]

In summary, we discovered a highly efficient doping method, ACTVIE, that is generally applicable to CSCPs, with one doped polymer achieving conductivities exceeding 350 S/cm and much improved stability. With further optimization in the molecular structure of CSCPs and doping conditions, the ACTVIE method will continue to offer novel conducting polymers for tailored applications.

■ ASSOCIATED CONTENT

Supporting Information

The Supporting Information is available free of charge at https://pubs.acs.org/doi/10.1021/jacs.4c09843.

Detailed experimental procedures including all syntheses and NMR spectra, conductivity measurement, Hall measurement, UPS/XPS spectra, FT-IR spectra, UV/vis absorption spectra, CV, and ToF-SIMS data (PDF)

■ AUTHOR INFORMATION

Corresponding Author

Wei You − *Department of Chemistry, University of North Carolina at Chapel Hill, Chapel Hill, North Carolina 27599, United States;* orcid.org/0000-0003-0354-1948; Email: wyou@unc.edu

Authors

Jordan Shanahan − *Department of Chemistry, University of North Carolina at Chapel Hill, Chapel Hill, North Carolina 27599, United States*

Liang Yan − *Department of Chemistry, University of North Carolina at Chapel Hill, Chapel Hill, North Carolina 27599, United States;* orcid.org/0000-0003-4122-7466

Yusuf Olanrewaju − *Department of Materials Science and Engineering, North Carolina State University, Raleigh, North Carolina 27695, United States*

Somayeh Kashani − *Department of Physics and ORaCEL, North Carolina State University, Raleigh, North Carolina 27695, United States*

Harald Ade − *Department of Physics and ORaCEL, North Carolina State University, Raleigh, North Carolina 27695, United States*

Franky So − *Department of Materials Science and Engineering, North Carolina State University, Raleigh, North Carolina 27695, United States;* orcid.org/0000-0002-8310-677X

https://doi.org/10.1021/jacs.4c09843
J. Am. Chem. Soc. 2024, 146, 32243−32248

Complete contact information is available at: https://pubs.acs.org/10.1021/jacs.4c09843

Author Contributions

The manuscript was written through contributions of all authors. All authors have given approval to the final version of the manuscript.

Notes

The authors declare the following competing financial interest(s): J.S. and W.Y. are inventors of a U.S. Provisional Patent Application No. 63/707,071 filed on October 14, 2024.

■ ACKNOWLEDGMENTS

All authors acknowledge the support from the Office of Naval Research (MURI Award N00014-23-1-2001). J.S. also acknowledges the support from the National Science Foundation (NSF) under Award DMR-2210586. A Bruker NEO 600 MHz NMR spectrometer was supported by NSF under Award CHE-1828183. The authors thank Dr. Marc A. ter Horst (UNC Chapel Hill Department of Chemistry NMR Core Laboratory) for the use of the NMR spectrometers. FT-IR, UPS, and XPS characterization was performed at the Chapel Hill Analytical and Nanofabrication Laboratory (CHANL), a member of the North Carolina Research Triangle Nanotechnology Network (RTNN), which is supported by NSF, Award ECCS-2025064, as part of the National Nanotechnology Coordinated Infrastructure (NNCI). Additionally, UPS and XPS of this work were performed using XPS/UPS/IPES instrumentation supported by the Center for Hybrid Approaches in Solar Energy to Liquid Fuels (CHASE), an Energy Innovation Hub funded by the U.S. Department of Energy, Office of Science, Office of Basic Energy Sciences under Award Number DE-SC0021173. We acknowledge Dr. Carrie Donley (CHANL) for the assistance with FT-IR, UPS, and XPS measurement. ToF-SIMS measurements were conducted at the Analytical Instrumentation Facility at NCSU, with partial support from the State of North Carolina and NSF. We acknowledge Chuanzhen (Elaine) Zhou for the assistance with the ToF-SIMS measurements.

■ REFERENCES

(1) Scaccabarozzi, A. D.; Basu, A.; Aniés, F.; Liu, J.; Zapata-Arteaga, O.; Warren, R.; Firdaus, Y.; Nugraha, M. I.; Lin, Y.; Campoy-Quiles, M.; Koch, N.; Müller, C.; Tsetseris, L.; Heeney, M.; Anthopoulos, T. D. Doping Approaches for Organic Semiconductors. *Chem. Rev.* **2022**, *122* (4), 4420−4492.

(2) Salzmann, I.; Heimel, G. Toward a Comprehensive Understanding of Molecular Doping Organic Semiconductors (Review). *J. Electron Spectrosc. Relat. Phenom.* **2015**, *204*, 208−222.

(3) Stanfield, D. A.; Wu, Y.; Tolbert, S. H.; Schwartz, B. J. Controlling the Formation of Charge Transfer Complexes in Chemically Doped Semiconducting Polymers. *Chem. Mater.* **2021**, *33* (7), 2343−2356.

(4) Kiefer, D.; Kroon, R.; Hofmann, A. I.; Sun, H.; Liu, X.; Giovannitti, A.; Stegerer, D.; Cano, A.; Hynynen, J.; Yu, L.; Zhang, Y.; Nai, D.; Harrelson, T. F.; Sommer, M.; Moulé, A. J.; Kemerink, M.; Marder, S. R.; McCulloch, I.; Fahlman, M.; Fabiano, S.; Müller, C. Double Doping of Conjugated Polymers with Monomer Molecular Dopants. *Nat. Mater.* **2019**, *18* (2), 149−155.

(5) Jacobs, I. E.; Lin, Y.; Huang, Y.; Ren, X.; Simatos, D.; Chen, C.; Tjhe, D.; Statz, M.; Lai, L.; Finn, P. A.; Neal, W. G.; D'Avino, G.; Lemaur, V.; Fratini, S.; Beljonne, D.; Strzalka, J.; Nielsen, C. B.; Barlow, S.; Marder, S. R.; McCulloch, I.; Sirringhaus, H. High-Efficiency Ion-Exchange Doping of Conducting Polymers. *Adv. Mater.* **2022**, *34* (22), 210298.

(6) Patel, S. N.; Glaudell, A. M.; Kiefer, D.; Chabinyc, M. L. Increasing the Thermoelectric Power Factor of a Semiconducting Polymer by Doping from the Vapor Phase. *ACS Macro Lett.* **2016**, *5* (3), 268−272.

(7) Jin, W.; Yang, C. Y.; Pau, R.; Wang, Q.; Tekelenburg, E. K.; Wu, H. Y.; Wu, Z.; Jeong, S. Y.; Pitzalis, F.; Liu, T.; He, Q.; Li, Q.; Huang, J. Da; Kroon, R.; Heeney, M.; Woo, H. Y.; Mura, A.; Motta, A.; Facchetti, A.; Fahlman, M.; Loi, M. A.; Fabiano, S. Photocatalytic Doping of Organic Semiconductors. *Nature* **2024**, *630*, 96−101.

(8) Yamashita, Y.; Tsurumi, J.; Ohno, M.; Fujimoto, R.; Kumagai, S.; Kurosawa, T.; Okamoto, T.; Takeya, J.; Watanabe, S. Efficient Molecular Doping of Polymeric Semiconductors Driven by Anion Exchange. *Nature* **2019**, *572* (7771), 634−638.

(9) Jacobs, I. E.; D'avino, G.; Lemaur, V.; Lin, Y.; Huang, Y.; Chen, C.; Harrelson, T. F.; Wood, W.; Spalek, L. J.; Mustafa, T.; O'keefe, C. A.; Ren, X.; Simatos, D.; Tjhe, D.; Statz, M.; Strzalka, J. W.; Lee, J. K.; Mcculloch, I.; Fratini, S.; Beljonne, D.; Sirringhaus, H. Structural and Dynamic Disorder, Not Ionic Trapping, Controls Charge Transport in Highly Doped Conducting Polymers. *J. Am. Chem. Soc.* **2022**, *144* (7), 3005−3019.

(10) Son, S. Y.; Lee, G.; Wang, H.; Samson, S.; Wei, Q.; Zhu, Y.; You, W. Integrating Charge Mobility, Stability and Stretchability within Conjugated Polymer Films for Stretchable Multifunctional Sensors. *Nat. Commun.* **2022**, *13*, 2739.

(11) Guo, C.; Quinn, J.; Sun, B.; Li, Y. An Indigo-Based Polymer Bearing Thermocleavable Side Chains for n-Type Organic Thin Film Transistors. *J. Mater. Chem. C* **2015**, *3* (20), 5226−5232.

(12) Liu, C.; Dong, S.; Cai, P.; Liu, P.; Liu, S.; Chen, J.; Liu, F.; Ying, L.; Russell, T. P.; Huang, F.; Cao, Y. Donor-Acceptor Copolymers Based on Thermally Cleavable Indigo, Isoindigo, and DPP Units: Synthesis, Field Effect Transistors, and Polymer Solar Cells. *ACS Appl. Mater. Interfaces* **2015**, *7* (17), 9038−9051.

(13) Ponder, J. F.; Gregory, S. A.; Atassi, A.; Menon, A. K.; Lang, A. W.; Savagian, L. R.; Reynolds, J. R.; Yee, S. K. Significant Enhancement of the Electrical Conductivity of Conjugated Polymers by Post-Processing Side Chain Removal. *J. Am. Chem. Soc.* **2022**, *144* (3), 1351−1360.

(14) Ponder, J. F.; Gregory, S. A.; Atassi, A.; Advincula, A. A.; Rinehart, J. M.; Freychet, G.; Su, G. M.; Yee, S. K.; Reynolds, J. R. Metal-like Charge Transport in PEDOT (OH) Films by Post-Processing Side Chain Removal from a Soluble Precursor Polymer. *Angew. Chem.* **2023**, *62*, e202211600.

(15) Zhao, H.; Shanahan, J. J.; Samson, S.; Li, Z.; Ma, G.; Prine, N.; Galuska, L.; Wang, Y.; Xia, W.; You, W.; Gu, X. Manipulating Conjugated Polymer Backbone Dynamics through Controlled Thermal Cleavage of Alkyl Side Chains. *Macromol. Rapid Commun.* **2022**, *43*, 2200533.

(16) Krebs, F. C. Design and Applications of Polymer Solar Cells with Lifetimes Longer than 10000 h. *Org. Photovoltaics VI* **2005**, *5938*, 59380Y.

(17) Søndergaard, R.; Helgesen, M.; Jørgensen, M.; Krebs, F. C. Fabrication of Polymer Solar Cells Using Aqueous Processing for All Layers Including the Metal Back Electrode. *Adv. Energy Mater.* **2011**, *1*, 68−71.

(18) Shanahan, J.; Oh, J.; Son, S. Y.; Siddika, S.; Pendleton, D.; O'Connor, B. T.; You, W. Strategic Incorporation of Cleavable Side Chains Improves Thermal Stability of PffBT-T4-Based Polymer Solar Cells. *Chem. Mater.* **2023**, *35* (23), 10139−10149.

(19) Manceau, M.; Helgesen, M.; Krebs, F. C. Thermo-Cleavable Polymers: Materials with Enhanced Photochemical Stability. *Polym. Degrad. Stab.* **2010**, *95* (12), 2666−2669.

(20) Liu, J.; Kadnikova, E. N.; Liu, Y.; McGehee, M. D.; Fréchet, J. M. J. Polythiophene Containing Thermally Removable Solubilizing Groups Enhances the Interface and the Performance of Polymer-Titania Hybrid Solar Cells. *J. Am. Chem. Soc.* **2004**, *126* (31), 9486−9487.

(21) Søndergaard, R. R.; Norrman, K.; Krebs, F. C. Low-Temperature Side-Chain Cleavage and Decarboxylation of Poly-

thiophene Esters by Acid Catalysis. *J. Polym. Sci. Part A Polym. Chem.* **2012**, *50* (6), 1127−1132.
(22) Kim, J.; Kim, J.; Lee, W.; Yu, H.; Kim, H. J.; Song, I.; Shin, M.; Oh, J. H.; Jeong, U.; Kim, T.; Kim, B. J. Tuning Mechanical and Optoelectrical Properties of Poly(3- Hexylthiophene) through Systematic Regioregularity Control. *Macromol. Res.* **2015**, *48*, 4339−4346.
(23) Seo, S.; Sun, C.; Lee, J.; Lee, S.; Lee, D.; Wang, C.; Phan, T. N.; Kim, G.; Cho, S.; Kim, Y.; Kim, B. J. Importance of High-Electron Mobility in Polymer Acceptors for Efficient All-Polymer Solar Cells : Combined Engineering of Backbone Building Unit and Regioregularity. *Adv. Funct. Mater.* **2022**, *32*, 2108508.
(24) Kim, Y.; Park, H.; Park, J. S.; Lee, J.; Kim, F. S.; Kim, H. J.; Kim, B. J. Regioregularity-Control of Conjugated Polymers: From Synthesis and Properties, to Photovoltaic Device Applications Youngkwon. *J. Mater. Chem. A* **2022**, *10*, 2672−2696.
(25) Lee, Y. W.; Pak, K.; Park, S. Y.; An, N. G.; Lee, J.; Kim, J. Y.; Woo, H. Y. Regioisomeric Polythiophene Derivatives : Synthesis and Structure- Property Relationships for Organic Electronic Devices. *Macromol. Res.* **2020**, *28* (8), 772−781.
(26) Pomerantz, M.; Amarasekara, A. S.; Dias, H. V. R. Synthesis and Solid-State Structures of Dimethyl 2, 2 ′ -Bithiophenedicarboxylates. *J. Org. Chem.* **2002**, *67* (20), 6931−6937.
(27) Heuvel, R.; Colberts, F. J. M.; Wienk, M. M.; Janssen, R. A. J. Thermal Behaviour of Dicarboxylic Ester Bithiophene Polymers Exhibiting a High Open-Circuit Voltage. *J. Mater. Chem. C* **2018**, *6* (14), 3731−3742.
(28) Son, S. Y.; Samson, S.; Siddika, S.; O'Connor, B. T.; You, W. Thermocleavage of Partial Side Chains in Polythiophenes Offers Appreciable Photovoltaic Efficiency and Significant Morphological Stability. *Chem. Mater.* **2021**, *33* (12), 4745−4756.
(29) Zhao, W.; Sun, J. Triflimide HNTf2) in Organic Synthesis. *Chem. Rev.* **2018**, *118*, 10349−10392.
(30) Nguyen, P. H.; Schmithorst, M. B.; Mates, T. E.; Segalman, R. A.; Chabinyc, M. L. Diffusion of Brønsted Acidic Dopants in Conjugated Polymers †. *J. Mater. Chem. C* **2023**, *11*, 7462−7470.
(31) Hofmann, A. I.; Kroon, R.; Yu, L.; Müller, C. Highly Stable Doping of a Polar Polythiophene through Co-Processing with Sulfonic Acids and Bistriflimide. *J. Mater. Chem. C* **2018**, *6* (26), 6905−6910.
(32) Salzmann, I.; Heimel, G.; Oehzelt, M.; Winkler, S.; Koch, N. Molecular Electrical Doping of Organic Semiconductors: Fundamental Mechanisms and Emerging Dopant Design Rules. *Acc. Chem. Res.* **2016**, *49* (3), 370−378.
(33) Wang, S.; Zhu, W.; Jacobs, I. E.; Wood, W. A.; Wang, Z.; Manikandan, S.; Andreasen, J. W.; Un, H. I.; Ursel, S.; Peralta, S.; Guan, S.; Grivel, J. C.; Longuemart, S.; Sirringhaus, H. Enhancing the Thermoelectric Properties of Conjugated Polymers by Suppressing Dopant-Induced Disorder. *Adv. Mater.* **2024**, *36*, 2314062.
(34) Hyun Suh, E.; Beom Kim, S.; Jung, J.; Jang, J. Extremely Electron-Withdrawing Lewis-Paired CN Groups for Organic p-Dopants. *Angew. Chem. Int. Ed.* **2023**, *62*, e202304245.
(35) Yi, H. T.; Gartstein, Y. N.; Podzorov, V. Charge Carrier Coherence and Hall Effect in Organic Semiconductors. *Sci. Rep.* **2016**, *6*, 23650.
(36) Wood, W. A.; Jacobs, I. E.; Spalek, L. J.; Huang, Y.; Chen, C.; Ren, X.; Sirringhaus, H. Revealing Contributions to Conduction from Transport within Ordered and Disordered Regions in Highly Doped Conjugated Polymers through Analysis of Temperature-Dependent Hall Measurements. *Phys. Rev. Mater.* **2023**, *7*, 034603.
(37) Scholes, D. T.; Yee, P. Y.; Lindemuth, J. R.; Kang, H.; Onorato, J.; Ghosh, R.; Luscombe, C. K.; Spano, F. C.; Tolbert, S. H.; Schwartz, B. J. The Effects of Crystallinity on Charge Transport and the Structure of Sequentially Processed F 4 TCNQ-Doped Conjugated Polymer Films. *Adv. Funct. Mater.* **2017**, *27*, 1702654.
(38) Chen, Y.; Yi, H. T.; Podzorov, V. High-Resolution Ac Measurements of the Hall Effect in Organic Field-Effect Transistors. *Phys. Rev. Appl.* **2016**, *5*, 034008.
(39) Aoyama, Y.; Yamanari, T.; Koumura, N.; Tachikawa, H.; Nagai, M.; Yoshida, Y. Photo-Induced Oxidation of Polythiophene Derivatives: Dependence on Side Chain Structure. *Polym. Degrad. Stab.* **2013**, *98* (4), 899−903.
(40) Gregory, S. A.; Hanus, R.; Atassi, A.; Rinehart, J. M.; Wooding, J. P.; Menon, A. K.; Losego, M. D.; Snyder, G. J.; Yee, S. K. Quantifying Charge Carrier Localization in Chemically Doped Semiconducting Polymers. *Nat. Mater.* **2021**, *20* (10), 1414−1421.
(41) Tan, J. K.; Png, R. Q.; Zhao, C.; Ho, P. K. H. Ohmic Transition at Contacts Key to Maximizing Fill Factor and Performance of Organic Solar Cells. *Nat. Commun.* **2018**, *9*, 3269.
(42) DeLongchamp, D. M.; Kline, R. J.; Lin, E. K.; Fischer, D. A.; Richter, L. J.; Lucas, L. A.; Heeney, M.; McCulloch, I.; Northrup, J. E. High Carrier Mobility Polythiophene Thin Films: Structure Determination by Experiment and Theory. *Adv. Mater.* **2007**, *19* (6), 833−837.
(43) Son, S. Y.; Samson, S.; Siddika, S.; O'Connor, B. T.; You, W. Thermocleavage of Partial Side Chains in Polythiophenes Offers Appreciable Photovoltaic Efficiency and Significant Morphological Stability. *Chem. Mater.* **2021**, *33* (12), 4745−4796.
(44) Zhao, H.; Shanahan, J. J.; Samson, S.; Li, Z.; Ma, G.; Prine, N.; Galuska, L.; Wang, Y.; Xia, W.; You, W.; Gu, X. Manipulating Conjugated Polymer Backbone Dynamics through Controlled Thermal Cleavage of Alkyl Side Chains. *Macromol. Rapid Commun.* **2022**, *43*, 2200533.

https://doi.org/10.1021/jacs.4c09843
J. Am. Chem. Soc. 2024, 146, 32243−32248